RESEARCH ARTICLE



Bomb pulse ¹⁴C evidence for consistent remodeling rates of cortical femur collagen in middle-late adulthood

Rhonda L. Quinn D

School of Earth, Environment and Society, Bowling Green State University, Bowling Green, Ohio, USA

Correspondence

Rhonda L. Quinn, School of Earth, Environment and Society, Bowling Green State University, 190 Overman Hall, Bowling Green, OH 43403. USA.

Email: rlquinn@bgsu.edu

Abstract

Objectives: Bomb pulse (BP) radiocarbon (¹⁴C) dating methods are used by forensic anthropologists to estimate the year-of-death (YOD) of unidentified individuals. Method resolution and accuracy depend on establishing lag times, or the difference between a tissue's BP ¹⁴C-derived year and the YOD, of various tissue types from known deceased persons. Bone lag times span many years and are thought to increase with age as a function of slowing remodeling rates. However, remodeling rates for various skeletal elements, bone structures and phases are not well known.

Materials and Methods: Here a simple method is used to estimate bone remodeling rates from a compilation of published cortical femur bone collagen BP 14 C measurements (n = 102). Linear regression models and nonparametric tests are used to detect changes in lag times and remodeling rates with increasing age-at-death.

Results: Remodeling rates and lag times of 3.5%/year and 29 years, respectively, are estimated from individuals aged 40–97 years. In contrast to previous work, the analysis yielded modest and negligible changes in remodeling rates and lag times with advancing age. Moreover, statistically significant differences in remodeling rates and lag times were not found between reported females and males.

Discussion: Implications for the temporal contexts within an individual's lifetime of biogeochemical data in archaeology and forensic anthropology are discussed, warranting additional BP ¹⁴C studies of known individuals and integration with histomorphometric analysis.

KEYWORDS

bomb pulse $^{14}\mathrm{C}$ dating, bone collagen remodeling rate, cortical femur collagen, lag time, year of death

1 | INTRODUCTION

1.1 | Determining year of death with bomb pulse ¹⁴C dating

Atmospheric radiocarbon (¹⁴C), emitted from above-ground testing of atomic bombs, rose exponentially from 1950 until circa 1963 with the start of testing ban agreements, then declined asymptotically toward pre-testing levels (Nydal, 1963; Nydal & Lövseth, 1970; Hua & Barbetti, 2004). ¹⁴C is incorporated into animal tissues via ingestion of

carbon-based foods such as plants and animals (Geyh, 2001; Stenhouse & Baxter, 1979). The continued measurement (Hua et al., 2013, 2021; Reimer et al., 2020) and resulting shapes of the atmospheric bomb pulse (BP) Δ^{14} C curves (denoted "BP curve") enable matching a calendar year range to an organism's tissue sample ¹⁴C value when formed after 1950 (Uno et al., 2013). Estimating a calendar year range of a bone or other tissue sample from a measured ¹⁴C value, reported as a fraction of modern ¹⁴C (denoted F¹⁴C), rests on a number of calculations and assumptions about the F¹⁴C measurement via Accelerated Mass Spectrometry (AMS) (Stenström et al., 2011). BP ¹⁴C dating

methods have been standardized and validated alongside the analytical growth and widespread use of AMS dating in archaeology (Taylor, 2000). Free and publicly available calibration software programs, such as OxCal (https://c14.arch.ox.ac.uk/oxcal) and Calibomb (http://calib.org/CALIBomb), enable users to calibrate a measured tissue F¹⁴C value and associated analytical error to location-specific BP curves, which yield calendar year ranges with associated probabilities.

BP ¹⁴C dating for determining the year of tissue death has broad applications including assessing tissue formation and subsequent activity (Bergmann et al., 2012; Lynnerup et al., 2008), modeling bone turnover (Hedges et al., 2007), tracking the illegal trade of elephant ivory (Cerling et al., 2016), and estimating the year of death (YOD) of unidentified individuals in forensic contexts (see reviews of Cook & MacKenzie, 2014; Ubelaker, 2014; Johnstone-Belford & Blau, 2020). When tissue death occurs. 14C uptake ceases, thus the F14C value serves as a proxy for the year of tissue death. However, the F14C-derived year of tissue death records an earlier interval than the actual time of the individual's death by weeks, months, or years; this delay is known as "lag time" (Broecker et al., 1959; Ubelaker & Buchholz, 2005). Depending on the tissue sampled, lag times can vary widely since the F¹⁴C value represents when ¹⁴C was incorporated via growth, repair or maintenance. These processes are constant but not necessarily uniform. occurring under specific circumstances and stages in life, which yield varying F¹⁴C values depending on tissue type as summarized below.

Blood and skin have relatively short lag times, suggesting the quick incorporation of new F¹⁴C values and replacement of previous F¹⁴C values (Hodgins, 2009). In contrast, tendons are slow to replace and can retain F¹⁴C values for many years (Heinemeier et al., 2013). Appositionally-growing tissues (e.g., hair, nails, and enamel) have F¹⁴C values that reflect their respective formation times throughout an individual's life (Hodgins, 2009). Thus the lag time is the equivalent of the time between tissue formation and an individual's death. Since hair and nails grow relatively quickly, but can preserve for a number of years after death, these tissues can provide accurate YOD estimations in forensic contexts (Johnstone-Belford et al., 2022a).

Tooth formation occurs during early-late childhood (Hillson, 1996), thus an enamel sample's lag time essentially spans most of an adult's lifetime. Enamel $F^{14}C$ values have been shown to approximate the year of crown growth completion and can be used to estimate an individual's year of birth (Alkass et al., 2011; Kondo-Nakamura et al., 2011; Spalding et al., 2005). Enamel neither remodels after formation (Hillson, 1996) nor continues to incorporate BP ^{14}C (Alkass et al., 2011; Hodgins, 2009); consequently, the $F^{14}C$ value is fixed to the year of birth and is not a direct proxy of YOD. However, if an unidentified individual's age-at-death is well constrained by other methods, an enamel $F^{14}C$ value can be used to estimate YOD simply by adding the determined age-at-death to the BP ^{14}C -derived year of birth (Ubelaker et al., 2006).

Bone lag times recorded in deceased individuals vary from years to decades depending on the age of the individual (Hodgins, 2009; Ubelaker et al., 2015). The BP year recorded in bone, denoted here as "bone year," represents the time when the bone underwent growth or last experienced remodeling. Different skeletal elements (e.g., long bones, vertebrae), bone structures (e.g., cortical vs. trabecular bone) and phases (collagen, bioapatite carbonate) have been shown to have

different lag times (Hodgins, 2009; Johnstone-Belford et al., 2022b; Ubelaker et al., 2022) likely reflecting dissimilar remodeling rates, which are related to form and function (Martin, 2000; Parfitt, 2002, 2004), diet (Kerstetter et al., 1999), activity and trauma (Ingle et al., 1999), osteoporosis (Fang et al., 2022), among other factors (Naylor et al., 2000; Robling et al., 2006; Stout & Lueck, 1995). But as pointed out in Johnstone-Belford and Blau (2020), bone remodeling rates are not well known due to a dearth of experimental work with known individuals

1.2 | Estimating bone remodeling rates with BP ¹⁴C dating methods

Bone remodeling rates in humans have been estimated with BP 14 C dating methods for some time (e.g., Geyh, 2001; Libby et al., 1964; Shin et al., 2004; Wild et al., 2000). Hedges et al. (2007) provided the first BP 14 C bone remodeling study of a large sample of well-documented deceased persons, spanning middle to late adulthood, and specific to skeletal element (femur), structure (cortical bone), and phase (bone collagen). This work upended the long-held understanding about the amount of time (\sim 10 years) represented with stable isotopic values of human bone, which are widely used in archaeology (Szpak et al., 2017) and increasingly used in forensic anthropology (Bartelink & Chesson, 2019). Hedges et al.'s (2007) remodeling rate estimations revealed that cortical femur bone collagen required a long time to completely remodel (i.e., 15+ years) and suggested that for middle-aged individuals there was a substantial amount of collagen retained from the adolescent period.

Hedges et al. (2007) used a bivariate plot of age-at-death and F¹⁴C values of 67 individuals to best-fit three bone turnover models tethered to four variables: birth (age 0), growth phase (age 10-20 years), cessation of growth (age 19-30 years), and death (age 100). Based on slope changes of F¹⁴C values with increasing age-at-death, the study also concluded that bone remodeling rates slowed with advancing age. Specifically, female bone remodeling rates were estimated to decrease from 4%/year at age 20 to 3%/year at age 80, whereas male bone remodeling rates were estimated at 3%/year at age 25 and decreased to 1.5%/year at age 80. This finding suggested that females have higher bone collagen remodeling rates than males during middle-late adulthood, but that males experience a steeper drop in remodeling rates with advancing age. Remodeling rates for individuals 10-15 years of age were estimated to be much higher, reported to between 5% and 30%/year. Notably, the individuals comprising the sample population had ages-at-death ≥40 years; consequently, the rate estimations during age <40 years relied on the turnover models instead of F14C values measured from known individuals within the younger age-at-death range.

Within the BP calendar year range, \sim 1950-today (Hua et al., 2021), determining a bone year is limited by the shape of the BP curve. That is, one F¹⁴C value yields two ranges of years, one on the ascending portion of the BP curve and the other on the descending portion (see Figure 1 for example of OxCal output). Although calibration program outputs include statistical probabilities for the calendar year

ranges on each of the two BP curve sides, determining the appropriate curve side typically requires an independent line of evidence, since bone lag times can extend beyond 30 years (Ubelaker et al., 2015). Utilizing OxCal to generate bone year ranges, a midpoint year for each sample on each side of the curve can be determined for F¹⁴C values (see the midpoint year use reported in Ubelaker and Parra, 2011).

Hedges et al. (2007) found a correlative relationship of decreasing F¹⁴C values with increasing age-at-death; Figure 2a reproduces Hedges et al.'s (2007) bivariate plot. Since F¹⁴C is a proxy for the year of tissue death, F¹⁴C values can be replaced with BP ¹⁴C-derived midpoint bone years derived from the ascending bomb curve and plotted against each individual's age-at-death (Figure 2b). The correlative relationship can be generally described as older individuals' bones were remodeled

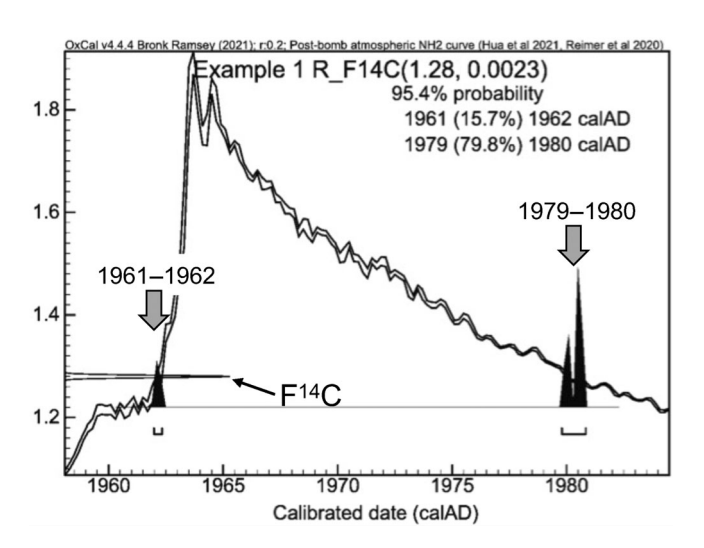


FIGURE 1 OxCal output of the bomb curve (NH Zone 2) position of a cortical femur bone collagen F¹⁴C value example showing two possible calendar year ranges.

during earlier years. Ubelaker et al. (2015) observed that Hedges et al. (2007) may have included bone collagen year ranges that derived from the descending portion of the BP curve. Replotting all bone year data from $F^{14}C$ values reported in Hedges et al. (2007) with years generated from both the ascending and descending curve illustrates the general shape of the BP curve (Figure 3a; Graphical Abstract). This graphic implies that if $F^{14}C$ values resided on the descending portion of the BP curve, the relationship between increasing age-at-death would be correlated to relatively later bone years, rather than earlier, altering the best-fit relationship found by Hedges et al. (2007).

But why does an individual's year-of-death necessarily matter when determining remodeling rates by age? Ideally the age of an individual when remodeling occurs is needed to estimate the length of time required for a bone to completely turnover. For individuals with a known birth year, the age of bone remodeling, denoted "bone age," can be calculated by subtracting the midpoint bone year from the individual's birth year. When the $F^{14}C$ value, or bone year, is translated to bone age for each individual reported by Hedges et al. (2007) from the ascending portion of the curve, there is a clear positive linear relationship with age-at-death (Figure 3b). Fitting a linear trendline to bone age versus age-at-death demonstrates a very strong ($R^2 = 0.99$) relationship in contrast to the large spread of raw $F^{14}C$ values with age-at-death (Figure 2a). Hedges et al. (2007) included individuals who died during different calendar years (1990–1993), which also may explain some of the variation in their plot.

The correlative relationship between bone age and age-at-death can be described as older individuals have older bones, and not surprisingly, suggests that remodeling continues to occur with advancing age. After Ubelaker et al.'s (2015) observation, bone ages from $F^{14}C$ values of Hedges et al. (2007) can also be derived from the descending portion of the curve (Figure 3b). The linear relationship is not as strong ($R^2=0.92$) and has a different slope and *y*-intercept, but the general relationship between age-at-death and bone age is the same.

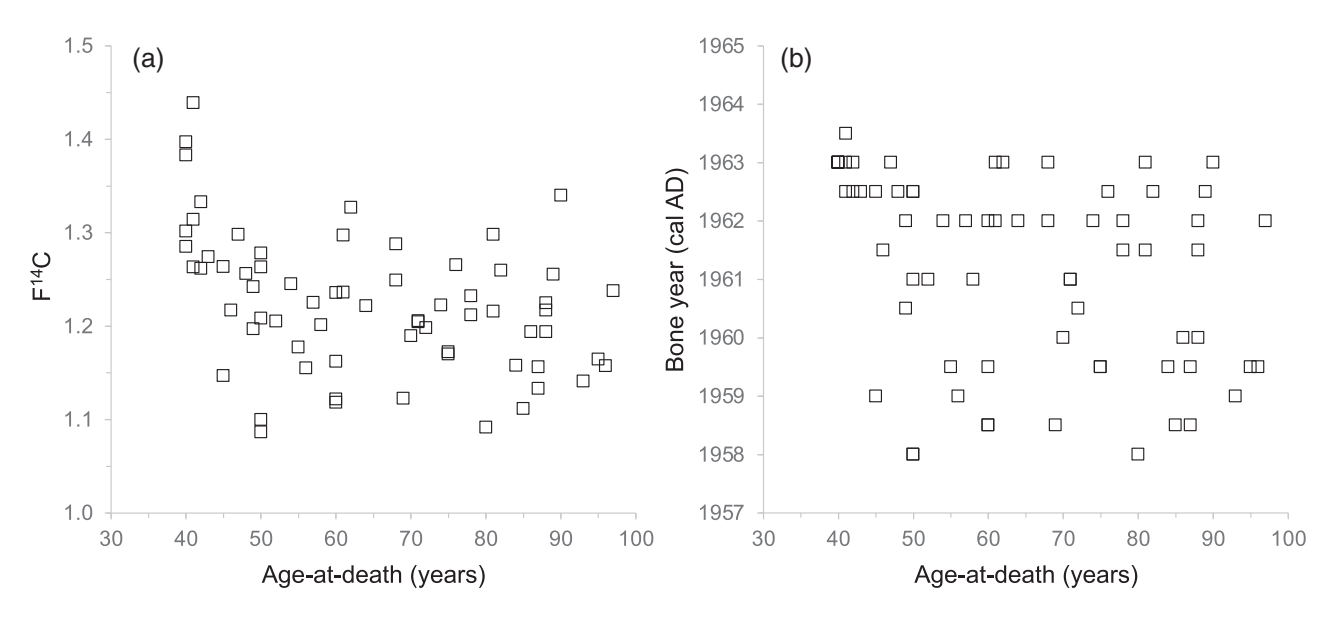


FIGURE 2 Bivariate plot of the (a) F¹⁴C value versus age-at-death and (b) bone year versus age-at-death of 67 individuals as reported in Hedges et al. (2007).

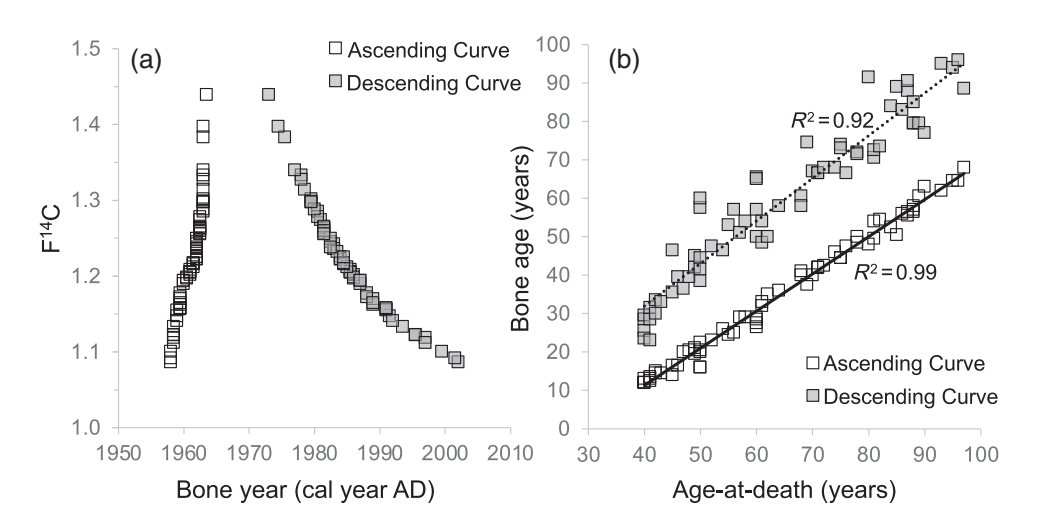


FIGURE 3 Bivariate plot of the (a) F¹⁴C values versus age-at-death and (b) bone age versus age-at-death of 67 individuals reported in Hedges et al. (2007) according to both ascending and descending portions of BP curve (SH Zone 1–2).

The variance differences between the two bone year versus age-atdeath relationships are an artifact of the BP curve shape, which produces relatively higher uncertainties on the descending portion as shown in Hodgins (2009) and mentioned in Johnstone-Belford et al. (2022b).

Hedges et al.'s (2007) models assumed steady state bone remodeling with the previous bone years considered to be "erased" by the most recent bone year. Thus the difference between bone age and age-at-death approximates the interval of time in years required for a bone to completely turnover, denoted here as "turnover interval." However, this represents the shortest interval of complete turnover, as death truncates the interval since the last time bone remodeling was recorded. A simple estimate of bone remodeling rate (%/year) after Parfitt (2002) is to determine the interval of time required to replace, or turnover, a bone completely. In equation form:

Remodeling rate (%per year) = 100% of bone \div turnover interval (years)
(1)

Because the turnover interval represents a minimum, Equation (1) results in a maximum remodeling rate. Although conceptually different, the turnover interval is the numeric equivalent of lag time, that is, the difference between bone age and age-at-death is equal to the difference between bone year and YOD. Consequently, if remodeling rates slow with age, lag times will increase with age. Throughout this study, "turnover interval" is replaced with the more commonly used "lag time" to minimize confusion.

1.3 | Approach of study

Since the publication of Hedges et al. (2007), additional cortical femur bone collagen $F^{14}C$ measurements of known individuals have been conducted (Johnstone-Belford et al., 2022b; Ubelaker et al., 2022), expanding the sample size, and importantly, contributing data from samples that can only date to one portion of the BP curve. To address the lack of useable data to estimate remodeling rates, published $F^{14}C$ values of cortical femur bone collagen of individuals with reported year-at-birth, age-at-death, year-at-death, and biological sex

assignment are compiled. Cortical femur bone collagen represents the largest element- and structure-specific sample from known deceased persons. From the compiled dataset, individuals whose $F^{14}C$ values can only be positioned on one side of the BP curve (n=28/107), a linear regression of bone age versus age-at-death is used to establish probable curve positions relative to a 95% confidence interval (CI) for all other samples. Making the determination between the two possible bone ages, on either the ascending or descending BP curve year range, rests on the assumption that individuals of the same age have comparable bone ages for cortical femur collagen.

Once the ascending or descending BP curve bone age is determined for each individual, all bone ages are used to calculate the lag time reported as whole number years. Equation (1) is then used to calculate remodeling rate (%/year) for all individuals. Based on the findings of Hedges et al. (2007), three main hypotheses are tested in this study: (H1) remodeling rates decrease with advancing age, (H2) females have faster absolute remodeling rates than males, and (H3) male remodeling rates decrease faster than those of females with advancing age. After Ubelaker et al. (2015), nonparametric comparisons are made between 10-year age-at-death groupings to detect changes in the three variables with advancing age. Several linear regression equations are generated utilizing age-at-death as the independent variable and bone age, lag time and remodeling rate serving as the dependent variable. Comparable nonparametric and linear regression analyses separated by reported biological sex assignments are also used to gauge bone remodeling rate differences between females and males. Table 1 lists each hypothesis tested in the study, variable predictions, statistical analyses and predicted outcomes, and associated labels and datasets included.

2 | MATERIALS AND METHODS

2.1 | Cortical femur bone collagen F¹⁴C compilation

The cortical femur bone collagen $F^{14}C$ data (Data S1) were taken from Hedges et al. (2007, n = 67), Ubelaker and Parra (2011, n = 4),

TABLE 1 Main hypotheses of study, variable predictions, statistical analyses and predicted outcomes, labels, and associated datasets used for analyses.

Main hypothesis	Variable predictions With increasing age-at- death	Statistical analyses: Predicted outcomes	Statistical analyses: Labels (sample size): Dataset(s)
H1: Remodeling rates slow with advancing age	H1-1: Bone age increases at relatively slower rate	Kruskal-Wallis one-way ANOVA of bone ages binned in 10-year age-at-death groups, $p < 0.05$ Mann-Whitney U -pairwise comparison yields decreasing median bone ages, $p < 0.05$ OLS regression: line slope <1, $R^2 > 0.5$, $p < 0.05$	Nonparametric comparisons (all data): Hedges H1-1, 2, 3 ($n = 67$): Hedges et al. (2007) Compilation H1-1, 2, 3 ($n = 102$): Hedges et al. (2007), Ubelaker and Parra (2011), Ubelaker et al. (2022), Johnstone-Belford et al. (2022b) OLS regressions (outliers removed): Hedges
	H1-2: Lag time increases	Kruskal-Wallis one-way ANOVA of lag times binned in 10-year age-at-death groups, $p < 0.05$ Mann-Whitney U -pairwise comparison yields decreasing median lag times, $p < 0.05$ OLS regression: line slope >0, $R^2 > 0.5$; $p < 0.05$	H1-1, 2, 3 (<i>n</i> = 64): Hedges et al. (2007) Compilation H1-1, 2, 3 (<i>n</i> = 90): Hedges et al. (2007), Ubelaker and Parra (2011), Ubelaker et al. (2022), Johnstone-Belford et al. (2022b)
	H1-3: Remodeling rate decreases	Kruskal-Wallis one-way ANOVA of remodeling rates binned in 10-year age-at-death groups, $p < 0.05$ Mann-Whitney U -pairwise comparison yields decreasing median remodeling rates, $p < 0.05$ OLS regression: line slope < 0 , $R^2 > 0.5$; $p < 0.05$	
H2: Females have higher remodeling rates than males	H2-1: Females have higher bone ages than males	Mann-Whitney U -pairwise comparisons of female and male bone ages: median female bone age > median male bone age, $p < 0.05$	Nonparametric comparisons (all data): Hedges H2-1, 2, 3 (females, $n=35$; males, $n=32$): Hedges et al. (2007)
	H2-2: Females have shorter lag times than males	Mann-Whitney <i>U</i> -pairwise comparisons of female and male lag times: median female lag time < median male lag time, <i>p</i> < 0.05	Compilation H2-1, 2, 3 (females, $n=44$; males, $n=56$): Hedges et al. (2007), Ubelaker et al. (2022), Johnstone-Belford et al. (2022b)
	H2-3: Females have higher remodeling rates than males	Mann-Whitney <i>U</i> -pairwise comparisons of female and male remodeling rates: median female remodeling rate > median male remodeling rate, <i>p</i> < 0.05	
H3: Male remodeling rates decrease with advancing age faster than females	H3-1: Female bone ages decrease less than males	OLS regressions of female and male bone ages: line slope: female > male, $R^2 > 0.5, p < 0.05$	OLS regressions (outliers removed): Hedges H2-1, 2, 3 (females, $n = 35$; males, $n = 32$):
	H3-2: Female lag times increase less than male lag times	OLS regressions of female and male lag times: line slope: female $<$ male, $R^2 > 0.5$, $p < 0.05$	Hedges et al. (2007) Compilation H2-1, 2, 3 (females, $n = 39$; males, $n = 49$): Hedges et al. (2007), Ubelaker et al.
	no-oo: remaie remodeling rates than male remodeling rates	OLD regressions of remains and male removering rates: line slope: female > male, $R^2 > 0.5$, $p < 0.05$	(2022), Johnstone-Belford et al. (2022b)

Ubelaker et al. (2022), n = 17), and Johnstone-Belford et al. (2022b, n=18). All but four of these individuals (reported in Ubelaker & Parra, 2011) have biological sex assignments. The vast majority of individuals range from 40 to 97 years of age at the time of death. The years of death are bimodally patterned ranging from 1984 to 2018. Two individuals, have an age-at-death of 16 and 21, respectively, and can be reliably assigned to the descending portion of the BP curve (reported in Ubelaker & Parra, 2011). Due to their potentially high remodeling rates, these two datapoints are excluded from determining BP curve position, nonparametric comparisons and OSL regression analysis, but are later discussed. Additionally, two reported datapoints yielded different bone years with the OxCal program relative to their F14C values: Individual 10 Case 39 (Ubelaker et al., 2022) and Donor 15 (Johnstone-Belford et al., 2022b). It is unknown if this was due to a typo in the reported F¹⁴C value or the reported midpoint year. These two datapoints are included in the Data S1 but excluded from the analysis.

2.2 | BP ¹⁴C determined bone years, bone ages, lag times, and remodeling rates

Based on the reported location and the F¹⁴C values of each bone collagen sample, OxCal (version 4.4, Bronk, 2021) was used to determine the year ranges on both the ascending and descending portions of the associated bomb curve (SH Zone 1–2). Comparable to methods of Ubelaker and Parra (2011), the midpoint bone year is determined, and used for calculating the bone age (i.e., midpoint bone year minus year-of-birth). Bone years are rounded to the nearest whole number (Data S1).

First, samples that can only reside on either the ascending or descending portion of the BP curve are selected. These include individuals whose (1) age at birth or pubescent growth stage (<10 years of age) postdate the bone age plotted on the ascending curve, (2) age-atdeath or year-at-death predate the bone age plotted on the descending curve. A linear (ordinary least squares, OLS) regression is made with bone age (dependent) versus age-at-death (independent) from these selected individuals, which demonstrate normality of residuals (Shapiro-Wilks W, p < 0.05). The two calculated bone ages of all other individuals based on the ascending and descending curves are plotted against the 95% upper and lower confidence limits of the regression equation. For each individual, the bone age that resides within the associated 95% CI and closest to the regression line is selected. From the determined BP curve placement bone age (midpoint bone year minus year-of-birth), lag time (equivalent of the age-at-death minus bone age) and remodeling rate (Equation 1) are calculated. Because a different approach is used to determine remodeling rate in this study, statistical comparisons are made with (1) only data taken from Hedges et al. (2007) and (2) the compilation dataset.

2.3 | Nonparametric statistical comparisons and linear regression analyses

Due to the availability of data from known deceased persons, neither the compilation dataset nor the data of Hedges et al. (2007) have normal distributions for age-at-death, bone age, lag time, or remodeling rate. Thus nonparametric tests (Kruskal-Wallis ANOVA, Mann-Whitney U-test) were used to detect statistically significant differences (p < 0.05) between all bone ages, lag times, and remodeling rates in 10-year age groups for the Hedges et al. (2007) dataset (n = 67) and for the compilation (n = 102). Likewise, Mann-Whitney U-pairwise comparisons were made between all individuals separated by reported biological sex assignments for the Hedges et al. (2007) dataset (female, n = 35; male, n = 32) and for the compilation dataset (female, n = 44; male, n = 56).

The OLS regression was chosen to gauge changes in the three variables with advancing age due to the strong, positive linear relationships found between bone age versus age-at-death in the data of Hedges et al. (2007) (Figure 3b). Homoscedasticity cannot be rejected for each of the variables (i.e., bone ages, lag times, remodeling rates) when regressed against age-at-death (Breusch-Pagan-Godfrey test, p > 0.05). However, Shapiro-Wilk W-tests and normal Q-Q plots of the residuals reveal skewness in both the Hedges et al. (2007) dataset and the compilation. Statistical outliers, defined as 1.5 \times interquartile range (IQR) of the remodeling rate, were removed to achieve normality of the residuals prior to OLR analysis. Since the data synthesized in this study are derived from biological systems, R² values greater than 0.6 are considered strong, and less than 0.2 are designated as weak; p-values < 0.05 are considered to reach statistical significance. Stat-Plus statistical software (v.7 AnalystSoft, Inc.) was used to conduct all statistical analyses.

3 | RESULTS

3.1 | Bomb curve placement and resulting bone ages, lag times, and remodeling rates

Based on the data points that could be assigned to either the ascending or descending side of the curve, the regression line illustrates the expected and strong positive relationship between bone age and ageat-death: Bone age = $-31.87 (\pm 1.61) + 1.01 (\pm 0.02) \times Age-at-death$ $(n = 28, R^2 = 0.99, p = 0.00)$ (Figure 4a). Separated by published datasets, Figure 4b-e illustrates where each individual's two bone ages plot relative to the regression line and 95% CI of the confident BP curve placements (Figure 4a). All of the ambiguous data reported from Hedges et al. (2007) that plot closest to the regression line derive from the ascending side of the BP curve (Figure 4b). From Ubelaker and Parra (2011), the two ambiguous data points from the ascending portion of the BP curve plot nearest to the line (Figure 4c). All descending portion data points from Ubelaker et al. (2022) and Johnstone-Belford et al. (2022b) plot closest to the line (Figure 4d,e). With curve placement established for all F¹⁴C values, all determined bone ages are plotted against age-at-death (Figure 4f), which constitute the compilation dataset.

Descriptive statistics of calculated lag times and remodeling rates for all individuals and separated by reported biological sex assignments are listed in Table 2. The calculated lag times and remodeling rates of Hedges et al.'s (2007) dataset and the compilation dataset

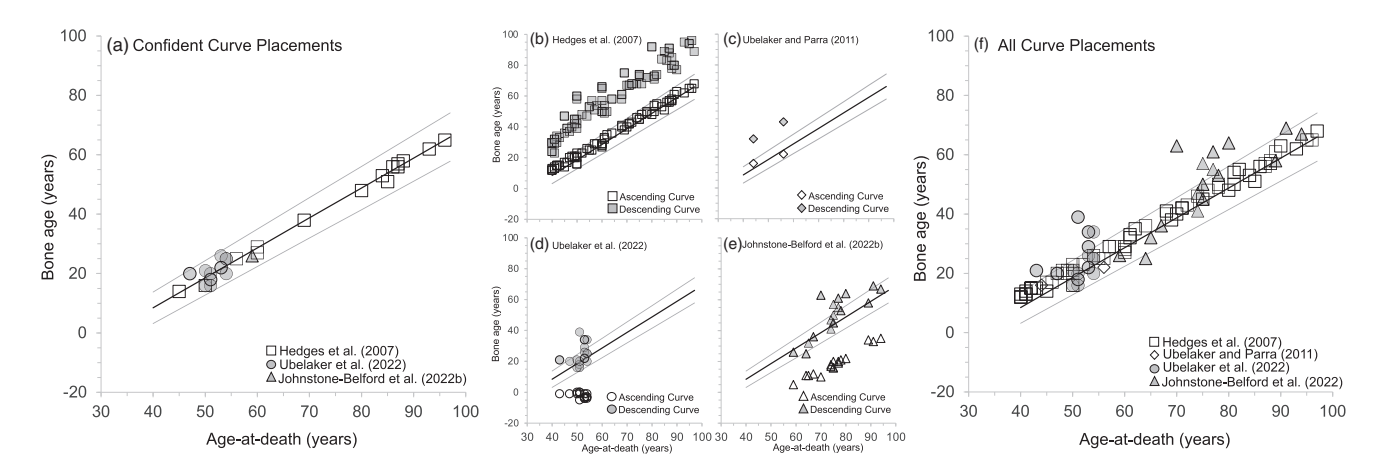


FIGURE 4 Linear regression of (a) confident bone ages versus age-at-death (black center line) and 95% CI (gray outer lines), (b-e) ascending and descending curve bone ages of all other datasets used in the compilation relative to confident bone age versus age-at-death regression line and 95% CI. (f) curve placement of all datapoints relative to regression line and 95% CI.

yielded comparable means and medians (Table 2). Notably, the compilation dataset shows higher variance likely because it includes bone ages derived from the descending BP curve. Prior to OLS regression analysis, three outliers were removed from the dataset of Hedges et al. (2007) and 12 outliers, from the compilation dataset. This achieved normality of the residuals (Shapiro–Wilk W, p > 0.05). Normal Q-Q plots of remodeling rates versus age-at-death are shown in Figure 5a–f. Descriptive statistics are provided for bone ages, lag times, and remodeling rates separated into 10-year age-at-death groupings for the Hedges et al. (2007) and compilation datasets (Tables 3 and 4).

3.2 | Nonparametric statistical comparisons

As expected, the median bone ages significantly increase between 10year age-at-death groupings (Kruskal-Wallis ANOVA, p < 0.05) in both datasets (Figure 6a, Hedges H1-1; 7A, Compilation H1-1). If remodeling rates slow with advancing age, bone ages would decrease incrementally across the 10-year age groups; however, this pattern was not found in either dataset (Table 5). Kruskal-Wallis One-way ANOVA of lag times and remodeling rates yield comparable statistical outcomes, since remodeling rate is derived from the numeric equivalent of lag time (see Equation 1). Mann-Whitney U-pairwise comparisons, as labeled in the remodeling rate box and whisker plots, yield statistically significant differences between several of the groups; however, there is no evidence for consistently increasing lag times (Figure 6b, Hedges H1-2; Figure 7b, Compilation H1-2) or consistently decreasing remodeling rates (Figure 6c, Hedges H1-3; Figure 7c, Compilation H1-3) with age-at-death. When each of the two datasets were separated into reported biological sex assignments, no statistically significant differences in pairwise comparisons were found between female and male bone ages (Figure 8a: Hedges H2-1, Compilation H2-1), lag times (Figure 8b: Hedges H2-2, Compilation H2-2) or remodeling rates (Figure 8c: Hedges H2-3, Compilation H2-3) when all age-atdeath data are combined. Consequently, with nonparametric statistical analyses of the complete Hedges et al. (2007, n=67) and compilation (n=102) datasets, H1-1, 2, 3, and H2-1, 2, 3 were rejected (Table 5).

3.3 | Linear regressions

Linear OLS regression equations for the data reported in Hedges et al. (2007) and the compilation dataset are illustrated in Figure 9a-f for all and unreported biological sex assignments and in Figure 10a-f when separated between reported females and males. Resulting regression equations, associated statistical outcomes, and tested hypothesis results are shown in Table 6. Regression equations derived from the plotted bone age versus age-at-death from individuals reported in Hedges et al. (2007) (Figure 9a), from the compilation dataset (Figure 9d), and when separated by reported biological sex assignments (Figure 10a,d) demonstrate strong, positive and highly significant linear relationships ($R^2 = 0.99$, p = 0.00). As expected, data derived from the descending portion of the BP curve show relatively higher variance, and thus, several outliers were identified and removed prior to OLS regression analysis. Outliers are shown in Figures 9a-f and 10a-f, denoted by a center dot.

Regression equation *Hedges* H1-1 yielded a line slope of 0.97, indicating that remodeling rates slightly slow with advancing age. The associated lag time and remodeling rate regression models, *Hedges* H1-2 and *Hedges* H1-3, yielded weak ($R^2 = 0.15$ and 0.16, respectively) but significant (p < 0.05) linear relationships with age-at-death. Utilizing the equation of *Hedges* H1-1, lag time is calculated to increase by 2 years (28 to 30 years) between the ages of 40 and 97. Remodeling rate changes as calculated with the equation of *Hedges* H1-3 results in a decrease in remodeling rate by 0.2% (3.6 to 3.4%/year) between ages 40 and 97. As a result, H1-1, 2, 3 cannot be rejected based on the analyses of Hedges et al.'s (2007) dataset. In contrast, the regression equation of *Compilation* H1-1 has a slope of

Mean (± standard deviation), median (± median absolute deviation), and maximum and IQRs of values of lag times and remodeling rates calculated for data reported in Hedges et al. (2007) and compilation dataset (data from Hedges et al., 2007; Ubelaker & Parra, 2011; Ubelaker et al., 2022; Johnstone-Belford et al., 2022b). TABLE 2

	Hedges et al. (2007) All data $(n = 67)$	Hedges et al. (2007) Females ($n=35$)	Hedges et al. (2007) Males ($n = 32$)	Compilation all data ($n=102$)	Compilation females ($n=44$)	Compilation males $(n = 56)$
Lag time mean (±σ)	29.3 ± 1.9 years	28.9 ± 1.4 years	29.7 ± 2.2 years	28.4 ± 4.6 years	27.8 ± 4.7 years	28.8 ± 4.4 years
Lag time median (±MAD)	29.0 ± 0.2 years	28.0 ± 0.2 years	29.0 ± 0.4 years	29.0 ± 0.5 years	$28.0 \pm 0.7 \text{ years}$	29.0 ± 0.6 years
Lag time maximum range	27-34 years	27-31 years	27-34 years	7-39 years	7-35 years	16-39 years
Remodeling rate average $(\pm \sigma)$	3.4 ± 0.2%/year	$3.5 \pm 0.2\%/year$	$3.4 \pm 0.2\%$ /year	3.7 ± 1.3 years	3.9 ± 1.8%/year	3.6 ± 0.7%/year
Remodeling rate median (±MAD)	3.5 ± 0.03%/year	3.6 ± 0.3%/year	3.5 ± 0.4%/year	3.5 ± 0.1 years	3.6 ± 0.3%/year	3.4 ± 0.1%/year
Remodeling rate maximum range	2.9-3.7%/year	3.2-3.7%/year	2.9-3.7%/year	2.6-14.3%/year	2.9-14.3%/year	2.6-6.3%/year
Remodeling rate IQR	2.72-4.08	3.21-3.93	3.40-3.96	2.75-4.16	3.16-3.98	2.75-4.16

0.99 indicating that remodeling rates negligibly slow between ages 40 and 97 years. The associated lag time and remodeling rate regression equations, Compilation H1-2 and Compilation H1-3, yielded very weak R^2 values and insignificant p-values (p > 0.05), which suggests that this is not a significant trend with age-at-death for either variable. Thus H1-1, 2, 3 were rejected based on the analyses of the compilation dataset (Table 6).

When separated into female and male groups, only the models utilizing the Hedges et al. (2007) dataset resulted in significant linear relationships (p < 0.05); however, R^2 values are weak (female $R^2 = 0.11$; male $R^2 = 0.13$). Using the Hedges H3-2 regression equations, female lag times increased from 28 to 29 years between the ages of 40 and 97. Male lag times increased from 29 to 32 years from ages 40 to 97. Using the Hedges H3-3 regression equations, female remodeling rates decrease from 3.6 to 3.4%/year from ages 40 to 97 years. Male remodeling rates are estimated to decrease from 3.6 to 3.3%/year between ages 40 and 97 years. According to the regression analyses of Hedges et al.'s (2007) dataset, H3-1, 2, 3 could not be rejected (Table 6), but the rate changes and differences between females and males are modest.

The Compilation H3-1 regression models produced strong, significant but similar linear relationships of females and males (Figure 10d. Table 6). Both the female and male regression equations have a slope of 0.98, indicating a slight slowing of remodeling rate with age-atdeath. Using the Compilation H3-2 and Compilation H3-3 regression equations for ages 40-97, female lag times increased from 28 to 30 years, and remodeling rates decreased from 3.5% to 3.4%/year. Male lag times increased from 30 to 31 years, and remodeling rates decreased from 3.4 to 3.3%/year. The different regression equation outputs suggests that females have slightly faster absolute remodeling rates by 0.1%, but the amount of slowing with advancing age is comparable to that of males. However, these lag time and remodeling rate regression models, yielded very weak R² values and insignificant pvalues (>0.5) suggesting the overall rate differences are negligible. Based on the regression analyses of compilation dataset, H3-1, 2, and 3 were rejected (Table 6).

4 | DISCUSSION

4.1 | Modest, negligible slowing of the remodeling rate during middle-late adulthood

BP ¹⁴C-derived bone ages of cortical femur bone collagen show a strong, positive linear relationship with age-at-death and provide the basis for assessing age-related bone remodeling rate changes. The results of this study based on the compilation dataset (n=102) and when outliers were removed (n=90) suggest that between 40 and 97 years of age, lag times do not significantly increase with advancing age for individuals \geq 40 years, but are consistent with a median of 29 years (95% CI = 25–35 years). The results presented here, however, do not imply that other skeletal elements, trabecular bone, or bioapatite phases remodel in a similar fashion as cortical

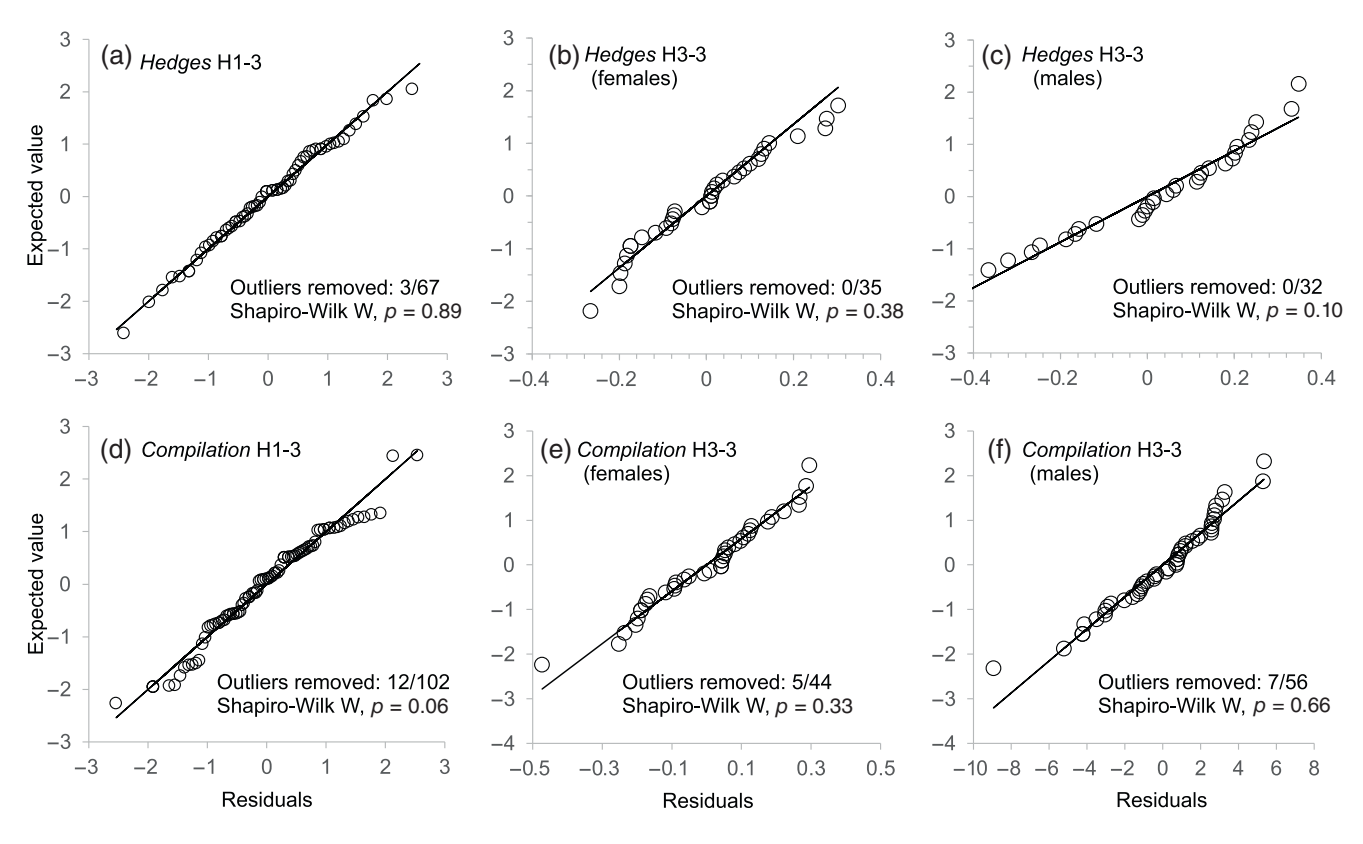


FIGURE 5 Representative normal Q-Q plots and Shapiro–Wilks W p-values illustrating normality of residuals after statistical outliers (1.5 × IQR) were removed from datasets used in the study.

femur bone collagen in terms of lag times, remodeling rates, or changes to both with age. Rather the study highlights the critical need for additional multi-element analyses of known individuals specific to structure and composition (e.g., Johnstone-Belford et al., 2022b; Ubelaker et al., 2022) for establishing remodeling rates and lag times to improve the utility of BP ¹⁴C-based YOD determinations.

Notably, the findings of this study are different than those of Ubelaker et al.'s (2015) meta-analysis of lag times derived from reported F¹⁴C values of various long bones. The authors concluded that lag times incrementally increased during middle-late adulthood based on 10-year age-at-death groups. For example, the largest agerelated increases of comparable age ranges were reported at 40-50 years old with an average lag time of 16.78 years, 50-60 years old with an average lag time of 25.42 years, and 60-70 years old with an average lag time of 31.63 years. But as recently demonstrated by Ubelaker et al. (2022) and Johnstone-Belford et al. (2022b), lag times should be determined for each skeletal element as well as bone structure (cortical vs. trabecular). Some of the long bone collagen F¹⁴C values compiled in Ubelaker et al. (2015) derived from both trabecular and cortical bone, as noted in Ubelaker et al. (2022). Moreover, based on the listed sample IDs (Table 1 in Ubelaker et al., 2015), it appears that different skeletal components (C: collagen, A: apatite, L: lipid) of anterior tibiae measured by Hodgins (2009) may have been included in the compiled dataset, which erroneously introduced lag time variability. As demonstrated by Hodgins (2009) these components within one skeletal element have different lag times, and thus likely different remodeling rates, within one individual.

A lag time range of 25-35 years, derived from the 95% CI of the Compilation H1-1 regression equation, is recommended for estimating YOD of a deceased person from cortical femur bone collagen when the individual is assigned an age-at-death ≥40 years. However, as mentioned previously, the spread of bone ages and relationship with age-at-death is influenced by the BP curve shape. F14C values positioned on the descending curve yield bone ages with higher uncertainties and resulted in several statistical outliers in the compilation dataset. For example, the largest outliers in bone remodeling rates were derived from 2002 to 2010 (cal year AD). Figure 11 illustrates that bone year increases with higher YOD, but with increasing spread of data from those years derived from the descending BP curve. The bimodal distribution of the compilation dataset demonstrates the need for additional method validation studies within the intermediate YOD range. Additionally, other factors may also contribute to the extreme outliers and requires further research with known individuals. For example, marine-based diets can result in incorporating older F¹⁴C values into bone collagen (Georgiadou & Stenström, 2010). Skeletal populations with known dietary contributions are warranted to quantify the impact on BP ¹⁴C dating methods.

4.2 | Modest, negligible remodeling rate differences between females and males

Separated by reported biological sex assignments, the results found in this approach are also different than previous work. As mentioned

Mean (± standard deviation), median (± median absolute deviation) and the range of values of bone ages, lag times, and remodeling rates by age-at-death 10-year groups calculated for the Hedges et al.'s (2007) dataset. TABLE 3

	Age-at-death: 40-49 years ($n=17$)	Age-at-death: $50-59$ years $(n=11)$	Age-at-death: 60- 69 years $(n = 11)$	Age-at-death: 70-79 years $(n=10)$	Age-at-death: 80-89 years ($n = 13$)	Age-at-death: 90-97 years $(n=5)$
Bone age mean (±σ)	$15.5 \pm 3.2 \text{ years}$	23.0 ± 4.5 years	33.5 ± 4.9 years	45.0 ± 3.3 years	54.8 ± 3.6 years	64.6 ± 2.3 years
Bone age median (±MAD)	15.0 ± 0.0 years	23.0 ± 0.0 years	33.0 ± 0.0 years	45.0 ± 0.5 years	56.0 ± 0.0 years	65.0 ± 0.0 years
Bone age range	12-21 years	16-29 years	27-41 years	40-50 years	48-61 years	62-68 years
Lag time mean (±σ)	27.9 ± 1.0 years	29.9 ± 2.3 years	29.5 ± 2.1 years	29.0 ± 0.8 years	$30.2 \pm 2.0 \text{ years}$	29.6 ± 1.7 years
Lag time median (±MAD)	28.0 ± 1.0 years	29.0 ± 0.0 years	29.0 ± 1.0 years	29.0 ± 1.0 years	31.0 ± 1.0 years	30.0 ± 0.0 years
Lag time range	27-31 years	27-34 years	27-33 years	28-30 years	27-34 years	27-31 years
Remodeling rate mean (±σ)	3.6 ± 0.1%/year	3.4 ± 0.2%/year	3.4 ± 0.2%/year	3.5 ± 0.1 years	$3.3 \pm 0.2\%/y$ ear	3.4 ± 0.2%/year
Remodeling rate median (±MAD)	3.6 ± 0.1%/year	3.5 ± 0.0%/year	3.5 ± 0.1%/year	3.5 ± 0.1%/year	$3.2 \pm 0.1\%$ /year	3.3 ± 0.0%/year
Remodeling rate range	3.2-3.7%/year	2.9-3.7%/year	3.0-3.7%/year	3.3-3.6%/year	2.9-3.7%/year	3.2-3.7%/year

TABLE 4 Mean (± standard deviation), median (± median absolute deviation) and the range of values of bone ages, lag times, and remodeling rates by age-at-death 10-year groups calculated for compilation dataset (data extracted from Hedges et al. (2007); Ubelaker and Parra (2011); Ubelaker et al. (2022); Johnstone-Belford et al. (2022b)).

	Age-at-death: $40-49$ years $(n=20)$	Age-at-death: 50-59 years ($n=27$)	Age-at-death: 60- 69 years ($n=14$)	Age-at-death: 70-79 years ($n=19$)	Age-at-death: 80–89 years ($n=15$)	Age-at-death: 90-97 years $(n=7)$
Bone age mean (±σ)	$16.1 \pm 3.3 \text{ years}$	23.9 ± 5.8 years	$32.9 \pm 5.0 \text{ years}$	48.5 ± 6.6 years	55.7 ± 4.1 years	65.6 ± 2.6 years
Bone age median (±MAD)	15.0 ± 3.0 years	23.0 ± 6.0 years	32.5 ± 3.0 years	47.0 ± 2.0 years	56.0 ± 0.0 years	65.0 ± 2.0 years
Bone age range	12-21 years	16-39 years	25-41 years	40-63 years	48-64 years	62-69 years
Lag time mean (±σ)	27.6 ± 1.6 years	29.0 ± 5.2 years	$30.6 \pm 3.2 \text{ years}$	25.9 \pm 6.3 years	29.3 ± 4.1 years	28.1 ± 3.2 years
Lag time median (±MAD)	28.0 ± 3.0 years	29.0 ± 5.0 years	31.0 ± 3.5 years	28.0 ± 2.0 years	31.0 ± 1.0 years	29.0 ± 2.0 years
Lag time range	22-31 years	12-35 years	27-39 years	7-33 years	16-34 years	22-31 years
Remodeling rate mean $(\pm \sigma)$	3.6 ± 0.2%/year	3.6 ± 1.1%/year	3.3 ± 0.3%/year	4.4 ± 2.5 years	3.5 ± 0.8%/year	3.6 ± 0.5%/year
Remodeling rate median (±MAD)	3.6 ± 0.5%/year	3.5 ± 0.7%/year	3.2 ± 0.4%/year	3.6 ± 0.2%/year	3.2 ± 0.1%/year	3.5 ± 0.3%/year
Remodeling rate range	3.2-4.6%/year	2.9-8.3%/year	2.6-3.7%/year	3.0–14.3%/year	2.9-6.3%/year	3.2-4.6%/year

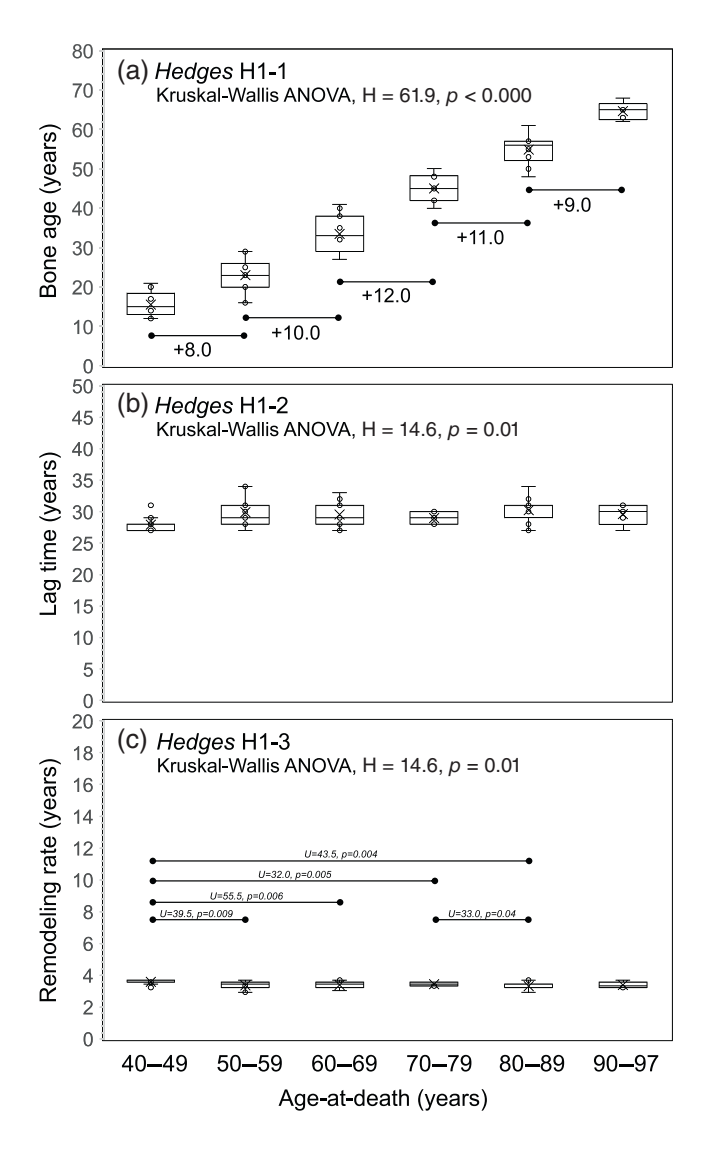


FIGURE 6 Box and whisker plots of the (a) bone ages, (b) lag times, and (c) remodeling rates grouped by 10-year intervals of ageat-death for Hedges et al.'s (2007) dataset. Statistically significant results of Kruskal–Wallis ANOVA for all three variables and pairwise comparisons for remodeling rate (Mann–Whitney *U*) are shown.

previously, Hedges et al. (2007) found female remodeling rates decreased from 4% to 3%/year from 20 to 80 years of age, and males, decreased from 3% to 1.5%/year from 25 to 80 years of age. The reanalysis of remodeling rates from only those data (*Hedges H1/H2/H3-1*, 2, 3) similarly resulted in significantly decreasing rates for both males and females but to a lesser extent than found by Hedges et al. (2007). Although cautioned due to a lack of data from the <40 age-at-death range, the *Hedges H3-3* regression equations are used to extrapolate to age-at-death 25 and 20 years for males and females, respectively, to compare directly to estimated rates of Hedges et al. (2007). Male remodeling rates decrease from 3.7 to 3.4%/year between ages 25–80 years. For females, remodeling rates decrease from 3.6 to 3.5%/year from ages 20–80 years. This alternate approach finds that the absolute remodeling rates of males and

females and the relative amount of slowing with age are more similar to one another. Importantly, these comparisons do not take into account the potential of different remodeling rates during early adulthood and prior to age 40 due to the lack of available data from younger individuals. Notably, nonparametric comparisons between pooled lag times and remodeling rates for all individuals in the Hedges et al. (2007) dataset did not yield statistically significant differences between females and males.

Similar slopes of the Compilation H3-1, 2, 3 regression models between males and females suggest that there are no age-related changes to lag times and remodeling rates. However, the two y-intercepts produce slightly different but substantially overlapping lag time ranges. From the Compilation H3-2 regression equations, the female lag time increases from 27 years (95% CI = 25-31 years) at the age of 40-29 years (95% CI = 25-34) at age 97. The male lag time increases from 27 years (95% CI = 24-35 years) at the age of 40-30 years (95% CI = 22-40) at age 97. Likewise, Compilation H3-3 showed that the 95% CI of female and male remodeling rates substantially overlap. Female remodeling rates span 3.2-3.9%/year at age 40 and 2.9-3.9%/year at age 97; male remodeling rates span 2.8-4.0%/year at age 40 and 2.3-3.3%/year at age 97. Importantly, neither the Compilation H3-2 or Compilation H3-3 regression equations reached statistical significance, suggesting that these modest age-related trends in male and female lag times and remodeling rates are negligible. Moreover, nonparametric comparisons between pooled lag times and remodeling rates for all ages in the compilation dataset did not yield statistically significant differences between females and males.

4.3 | Adolescent and early adulthood remodeling rates

Utilizing the two individuals with young age-at-death years (reported in Ubelaker and Parra, 2011) to calculate bone remodeling rates with Equation (1) results in much higher remodeling rates during adolescence and early adulthood, as expected. The individual with an ageat-death of 16 years yielded a BP bone age of 13 years, resulting in a maximum remodeling rate of 33%/year. The individual with an age-atdeath of 27 years has a BP bone age of 15, which equates to a remodeling rate of 8%/year. But as mentioned previously, Equation (1) estimates the maximum rate possible, as the young age-at-death simply truncates the time since growth experienced during adolescence. Plotting these two datapoints with all other data illustrates a declining rate change pattern (Figure 12), which generally follows the models of Hedges et al. (2007). To date, lag times of cortical femur bone collagen from individuals with age-at-death <40 years are not well known (Ubelaker et al., 2015), which can result in interpretative problems for year-of-death estimations based on BP ¹⁴C dating methods. Analyses of identified individuals representing the younger age ranges are needed to properly estimate adolescent and early adulthood remodeling rates and the timing of expected rate changes.

TABLE 5 Nonparametric statistical outcomes, dataset-hypothesis label and figure number for each variable prediction.

Hypothesis: With increasing age-at-death	Figure	Dataset-hypothesis label: nonparametric statistical outcomes	Hypothesis test result
H1-1: Bone age increases at relatively slower rate	Figure 6a	Hedges H1-1: 10-year group Kruskal–Wallis ANOVA, H = 61.9 , $p < 0.000$; median bone age differences increase from $40-50$ years to $60-70$ years, decrease from $60-70$ years to $70-80$ years	Rejected
	Figure 7a	Compilation H1-1: 10-year group Kruskal–Wallis ANOVA, H = 90.5, $p = 0.000$; median bone age differences increase from 40–50 years to 60–70 years, decrease from 60–70 years to 70–80 years	Rejected
H1-2: Lag time increases	Figure 6b	Hedges H1-2: 10-year group Kruskal–Wallis ANOVA, H = 14.6, $p = 0.01$; Mann–Whitney U -pairwise comparisons show between group lag times fluctuate with age-at-death	Rejected
	Figure 7b	Compilation H1-2: 10-year group Kruskal–Wallis ANOVA, $H=16.8$, $p=0.005$; Mann–Whitney U -pairwise comparisons show between group lag times fluctuate with age-at-death	Rejected
H1-3: Remodeling rate decreases	Figure 6c	Hedges H1-3: 10-year group Kruskal–Wallis ANOVA, H = 14.6, $p = 0.01$; Mann–Whitney U-pairwise comparisons show between group remodeling rates fluctuate with age-at-death	Rejected
	Figure 7c	Compilation H1-3: 10-year group Kruskal–Wallis ANOVA, H = 16.8, $p = 0.005$; Mann–Whitney U-pairwise comparisons show between group remodeling rates fluctuate with age-at-death	Rejected
H2-1: Females have higher bone ages than males	Figure 8a	Hedges H2-1: Mann–Whitney U -pairwise comparisons of female and male bone ages, $U=450$, two-tailed p -value = 0.17	Rejected
		Compilation H2-1: Mann–Whitney U-pairwise comparisons of female and male bone ages, $U = 1142$, two-tailed p-value = 0.53	Rejected
H2-2: Females have shorter lag times than males	Figure 8b	Hedges H2-2: Mann–Whitney U -pairwise comparisons of female and male lag times, $U=453.5$, two-tailed p -value $=0.18$	Rejected
		Compilation H2-2: Mann–Whitney U -pairwise comparisons of female and male lag times, $U = 1064$, two-tailed p -value = 0.24	Rejected
H2-3: Females have higher remodeling rates than males	Figure 8c	Hedges H2-3: Mann–Whitney U -pairwise comparisons of female and male remodeling rates, $U=453.5$, two-tailed p -value $=0.18$	Rejected
		Compilation H2-3: Mann–Whitney U-pairwise comparisons of female and male remodeling rates, $U=1064$, two-tailed p-value = 0.24	Rejected

 $\it Note$: Refer to Table 1 for associated dataset(s). Statistically significant $\it p$ values are shown in bold.

4.4 | Lifetime representation and time-averaging of bone collagen biogeochemical measurements

Aspects of diet, residential mobility, health, and status are regularly inferred from isotopic values and elemental concentrations measured from human bone in archaeology (e.g., Koon & Tuross, 2013; Lamb et al., 2014; Reitsema & Vercellotti, 2012) and forensic anthropology (Lehn et al., 2015; Meier-Augenstein & Fraser, 2008; Quinn et al., 2021). Bone remodeling rates provide the foundations for interpreting how much time of an individual's life is represented with

biogeochemical measurements (e.g., Cox & Sealy, 1997; Fahy et al., 2017; Lamb et al., 2014; Scharlotta et al., 2013; Sealy et al., 1995). This study finds that adolescent growth dominates the cortical femur bone collagen F¹⁴C signal well into middle adulthood, aligned with the interpretation of Geyh (2001) and modeled by Hedges et al. (2007). For example, at face value, the relationship between bone age and age-at-death implies that cortical femur bone collagen of a middle-aged individual (40 years old) records information about the individual during adolescence (11 years old). Hedges et al. (2007) delineated age ranges to characterize the adolescent period of

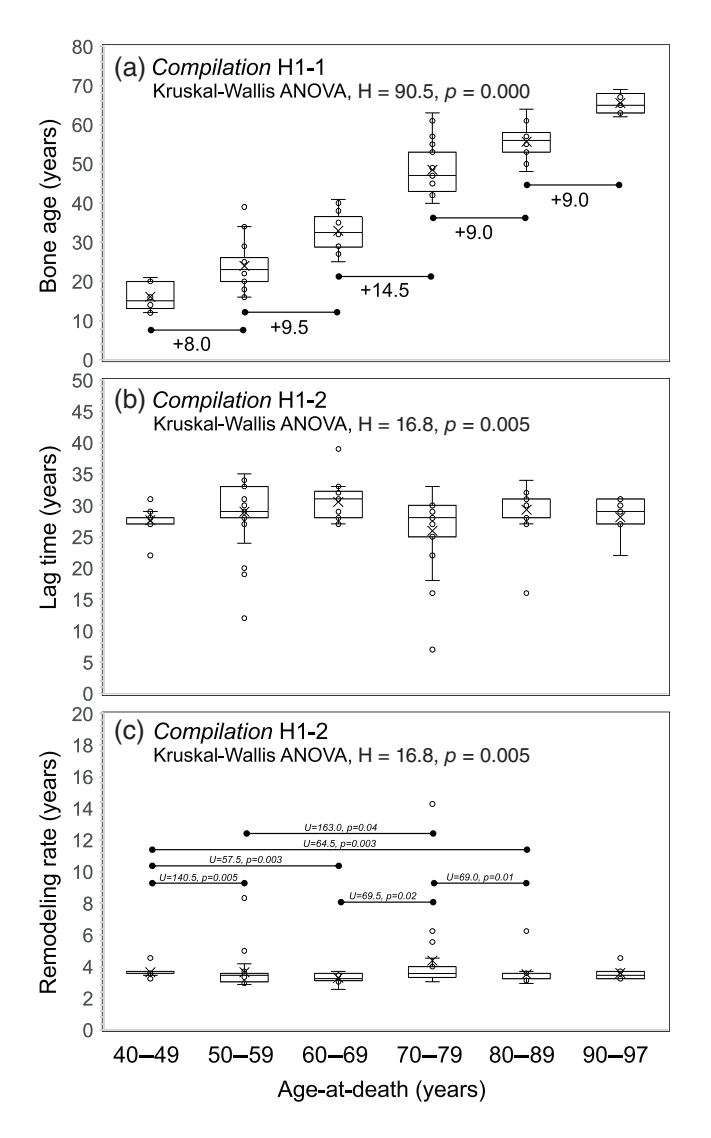


FIGURE 7 Box and whisker plots of the (a) bone ages, (b) lag times, and (c) remodeling rates grouped by 10-year intervals of ageat-death for the compilation dataset. Statistically significant results of Kruskal–Wallis ANOVA for all three variables and pairwise comparisons for remodeling rate (Mann–Whitney *U*) are shown.

growth (10–19 years) and the early adulthood period of cessation (20–30 years). The results here, incorporating additional data of identified individuals, indicate that the average age threshold for "erasing" the adolescent period of growth, that is, recording a bone age of 20 years, is not reached until 49 years of age.

As shown by histomorphometric analysis (Gocha & Agnew, 2016), cortical femur bone collagen is an average of an extremely wide range of time, represented by different ages of bone, some retained since puberty and others remodeled throughout an individual's lifetime. However, as shown here, one F¹⁴C value of cortical femur bone collagen is calculated to a relatively discrete year range. Thus it is not clear from BP ¹⁴C dating alone whether cortical femur bone collagen represents (1) an average of many years, incorporating all bone remodeled from the age-of-death and extending to 25–35 years prior to death or (2) a more limited interval (3, 5, 10 years?) during a previous time period during the individual's life (~25–35 years prior to death). This

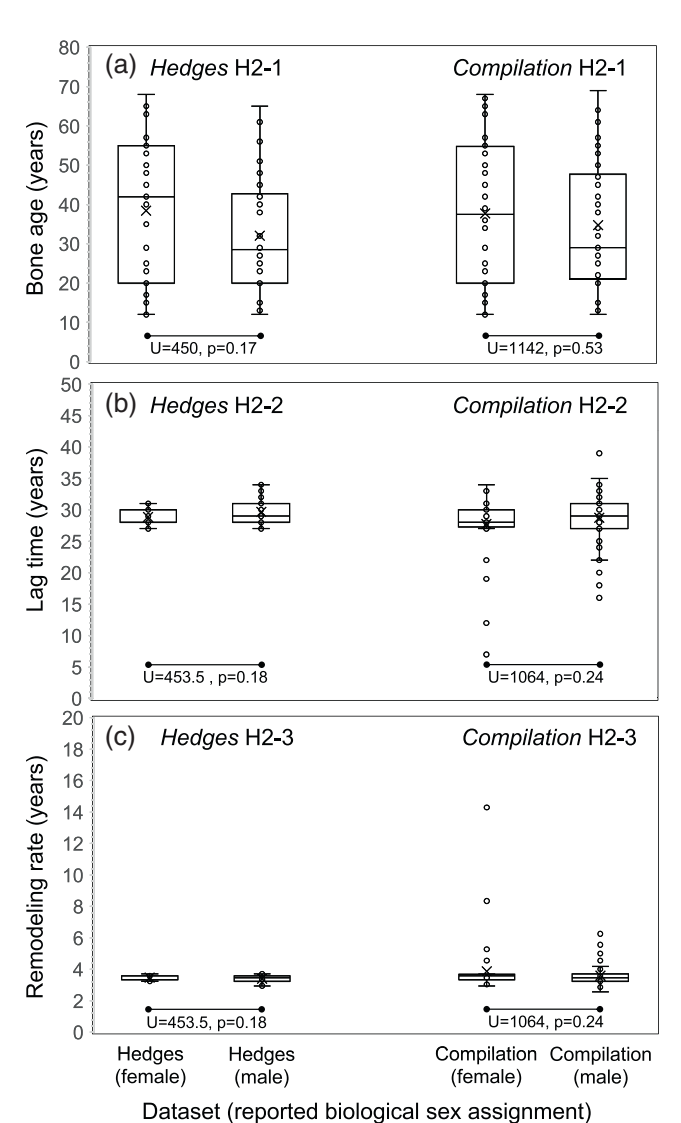


FIGURE 8 Box and whisker plots and results of the Mann-Whitney *U*-tests comparing female and male (a) bone ages, (b) lag times, and (c) remodeling rates for the Hedges et al.'s (2007) dataset and the compilation dataset.

lack of temporal resolution potentially impacts interpretations of biogeochemical data in archeological contexts for inferring lifeways and is especially concerning for geoprofiling used to aid in the identification of unknown individuals in forensic contexts (Bartelink & Chesson, 2019). Higher resolution sampling (Matsubayashi & Tayasu, 2019), F¹⁴C uptake modeling (Bernard et al., 2010), and data integration from multiple lines of evidence for bone remodeling rates and patterns (Fahy et al., 2017) are warranted to better constrain the amount and interval of a lifetime recorded in bone.

5 | CONCLUSION

A simple method for calculating the bone remodeling rates from BP ¹⁴C analysis is presented and used to revisit the study of Hedges et al. (2007). By synthesizing published F¹⁴C values of cortical femur bone

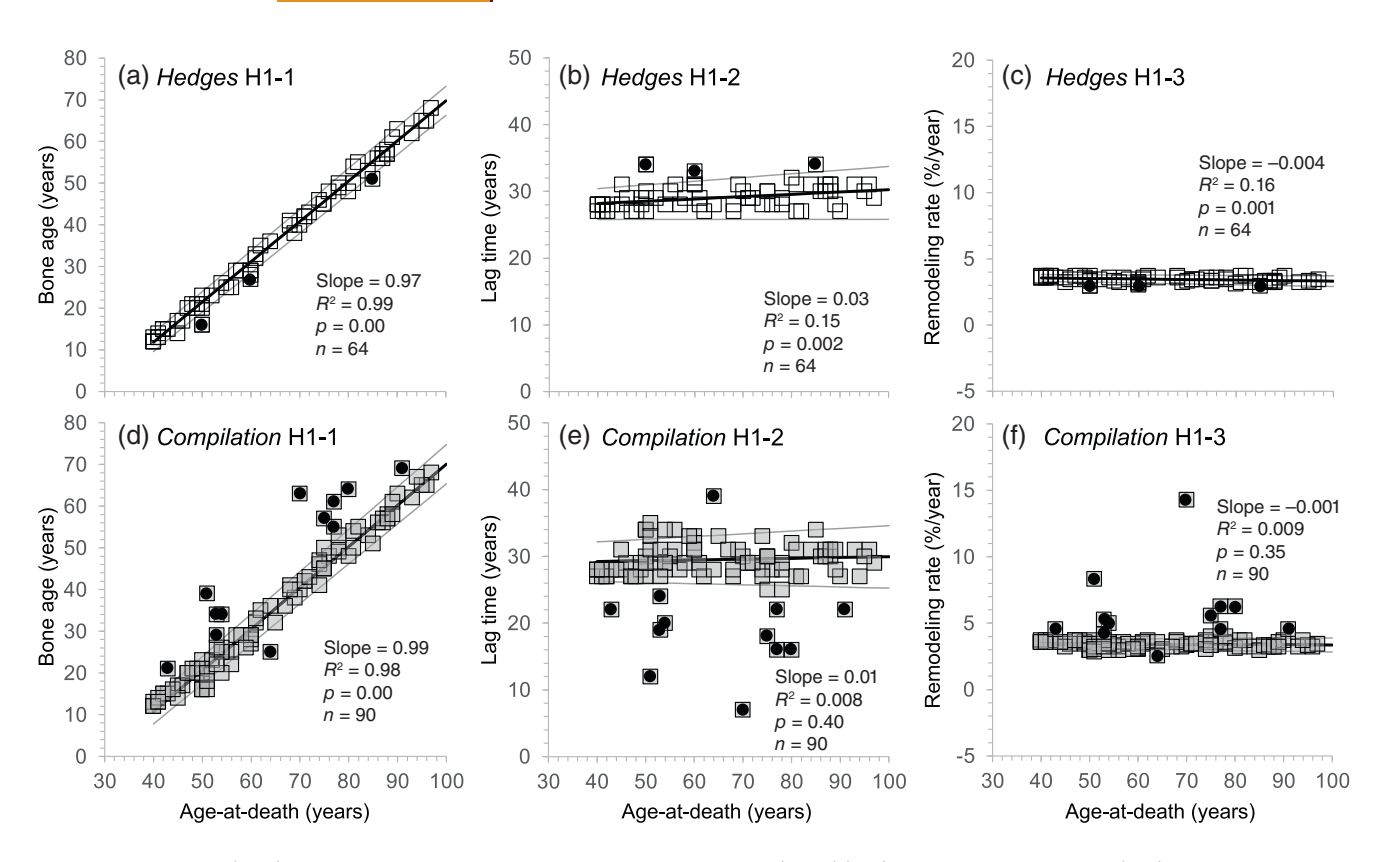


FIGURE 9 Linear (OLS) regression equations of the data from Hedges et al.'s (2007) (a-c) and compilation dataset (d-f).

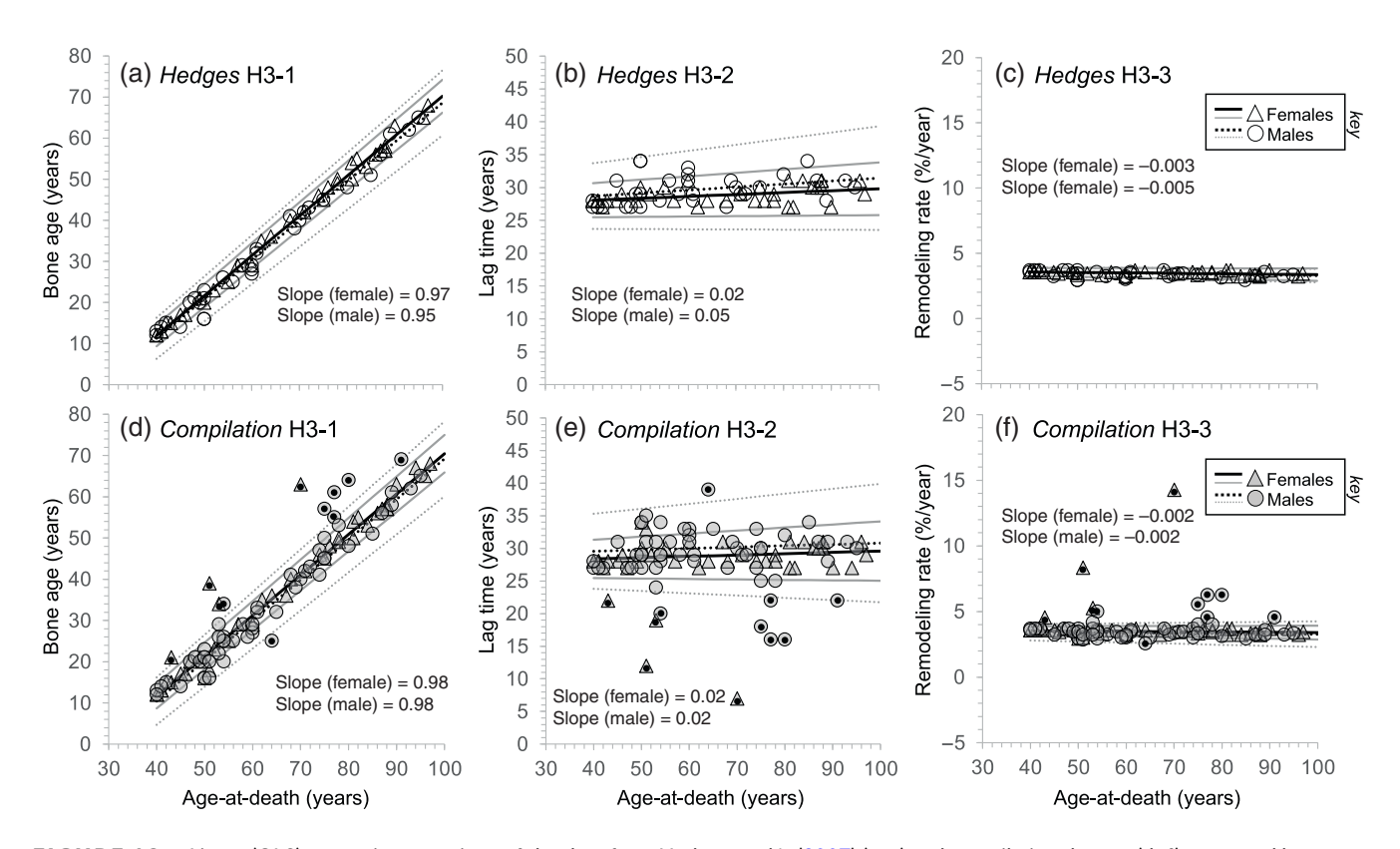


FIGURE 10 Linear (OLS) regression equations of the data from Hedges et al.'s (2007) (a-c) and compilation dataset (d-f) separated by reported biological sex assignments.

TABLE 6 Linear (OLS) regression equation(s) and the statistical outcome(s), dataset-hypothesis label and figure number for each variable prediction.

rediction.			
Hypothesis: With increasing age-at-death	Figure	Dataset-hypothesis label: OLS regression equation(s) and statistical outcomes	Hypothesis test result
H1-1: Bone age increases at relatively slower rate	Figure 9a	Hedges H1-1: Bone age (years) = -26.79 (±0.70) + 0.97 (±0.01) × Age-at-death (years) (n = 64, $R^2 = 0.99$, $p = 0.00$)	Cannot reject
	Figure 9d	$\begin{aligned} & \textit{Compilation H1-1: Bone age (years)} = -28.74 \ (\pm 0.94) \\ & + 0.99 \ (\pm 0.01) \times \text{Age-at-death (years)} \ (\textit{n} = 90, \\ & R^2 = 0.98, \textit{p} = \textbf{0.00}) \end{aligned}$	Rejected
H1-2: Lag time increases	Figure 9b	$\label{eq:hedges} \begin{aligned} &\text{Hedges H1-2: Lag time (years)} = 26.79~(\pm0.70) + 0.03\\ &(\pm0.01) \times \text{Age-at-death (years)}~(n=64;~R^2=0.15;\\ &\textit{p}=0.002) \end{aligned}$	Cannot reject
	Figure 9e	Compilation H1-2: Lag time (years) = 28.74 (±0.94) + 0.01 (±0.01) × Age-at-death (years) (n = 90, R^2 = 0.01, p = 0.40)	Rejected
H1-3: Remodeling rate decreases	Figure 9c	Hedges H1-3: Remodeling rate (%/year) = 3.72 (± 0.08) - 0.004 (± 0.001) \times Age-at-death (years) ($n=64$; $R^2=0.16$; $p=0.001$)	Cannot reject
	Figure 9f	Compilation H1-3: Remodeling rate (%/year) = 3.50 (\pm 0.10) - 0.002 (\pm 0.002) \times Age-at-death (years) ($n=90, R^2=0.001, p=0.35$)	Rejected
H3-1: Female bone ages decrease less than male bone ages	Figure 10a	Hedges H3-1: Female bone age (years) = -26.9 (± 0.81) + 0.97 (± 0.01) × age-at-death (years) ($n=35$, $R^2=0.99$, $p=0.00$); Male bone age (years) = -26.9 (± 1.50) + 0.95 (± 0.02) × age-at-death (years) ($n=32$, $R^2=0.99$, $p=0.00$)	Cannot reject
	Figure 10d	Compilation H3-1: Female bone age (years) = -27.59 (± 0.92) + 0.98 (± 0.01) × age-at-death (years) ($n=39$, $R^2=0.99$, $p=0.00$); Male bone age (years) = -28.71 (± 1.76) + 0.98 (± 0.03) × age-at-death (years) ($n=49$, $R^2=0.96$, $p=0.00$)	Rejected
H3-2: Female lag times increase less than male lag times	Figure 10b	$\label{eq:hedges} \begin{array}{l} \textit{Hedges} \ \mbox{H3-2: Female lag time (years)} = 26.9 \ (\pm 0.81) \\ + \ \ \mbox{0.02} \ (\pm 0.01) \times \mbox{age-at-death (years)} \ (n = 35, \\ \ \ \mbox{$R^2 = 0.16$, $p = 0.02$);} \ \mbox{Male lag time (years)} = 26.9 \\ \ \ \mbox{$(\pm 1.50) + 0.05$ $(\pm 0.02) \times $age-at-death (years)$} \\ \ \ \mbox{$(n = 32$, $R^2 = 0.11$, $p = 0.06$)} \end{array}$	Cannot reject
	Figure 10e	Compilation H3-2: Female lag time (years) = 27.59 (± 0.92) + 0.02 (± 0.01) × age-at-death (years) ($n=39$, $R^2=0.06$, $p=0.14$); Male lag time (years) = 28.71 (± 1.76) + 0.02 (± 0.03) × age-at-death (years) ($n=49$, $R^2=0.01$, $p=0.45$)	Rejected
H3-3: Female remodeling rates decrease less than male remodeling rates	Figure 10c	Hedges H3-3: Female remodeling rate (%/year) = 3.69 (± 0.10) $- 0.003$ (± 0.001) \times age-at-death (years) ($n=35, R^2=0.15, p=0.02$); Male remodeling rate (%/year) = 3.72 (± 0.16) $- 0.005$ (± 0.002) \times age-at-death (years) ($n=32, R^2=0.13, p=0.04$)	Cannot reject
	Figure 10f	Compilation H3-3: Female remodel rate (%/year) = $3.62 (\pm 0.11) - 0.002 (\pm 0.002) \times$ age-at-death (years) (n = 39 , $R^2 = 0.06$, $p = 0.14$); Male remodel rate (%/year) = $3.51 (\pm 0.19) + 0.002$ ($\pm 0.003) \times$ age-at-death (years) (n = 49 , $R^2 = 0.01$, $p = 0.42$)	Rejected

 $\it Note$: Refer to Table 1 for associated dataset(s). Statistically significant $\it p$ values are shown in bold.

collagen from 102 deceased individuals with known year-of-birth, year-of-death, and age-at-death, linear (OLS) regression models showed that lag time (i.e., the time between tissue death and YOD) does not change with advancing age, but consistently equals 29 years

(95% CI = 25-35 years) after the age of 40. Using lag time to estimate bone remodeling rate (see Equation 1) yielded a consistent rate of 3.5%/year between ages 40-97. Separated by reported biological sex assignments, changes in lag times and remodeling rates with

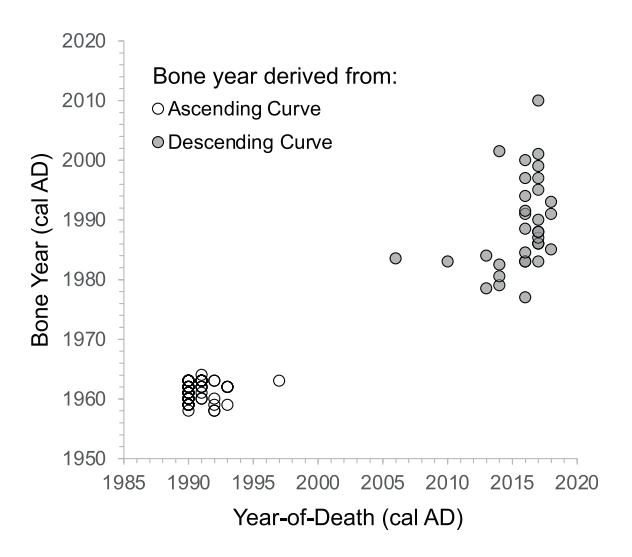


FIGURE 11 Bivariate plot of the bone year versus year-of-death for all individuals in compilation dataset (n = 102).

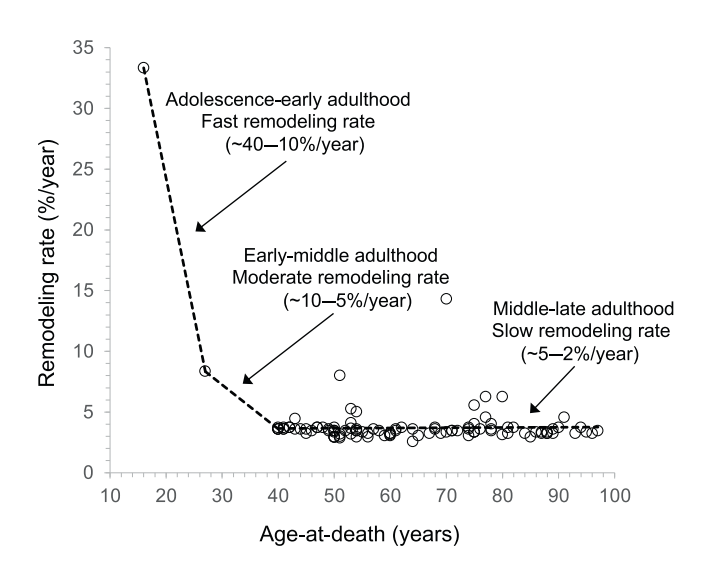


FIGURE 12 Bivariate plot of the remodeling rate versus ageat-death for compilation dataset and two young individuals (data taken from Ubelaker & Parra, 2011). Linear trendlines are fitted to illustrate the three age-related remodeling rate changes.

advancing age were comparable for females and males. In summary, with current F¹⁴C data, there is little evidence that remodeling rates of cortical femur bone collagen slow with age during middle-late adulthood or show statistically significant differences between females and males. Additional F¹⁴C measurements of known individuals are warranted, especially from those with BP ¹⁴C-derived bone years that can only be positioned on either the ascending or descending portion of the BP curve and representing age ranges during adolescence and young adulthood.

AUTHOR CONTRIBUTIONS

Rhonda L. Quinn: Conceptualization (lead); data curation (lead); formal analysis (lead); investigation (lead); methodology (lead); project administration (lead); resources (lead); software (lead); supervision (lead);

validation (lead); visualization (lead); writing – original draft (lead); writing – review and editing (lead).

ACKNOWLEDGMENTS

The author is thankful for the anonymous critiques generously provided by two reviewers and an editorial board member that greatly improved previous manuscript drafts. This work was inspired by collaborations with Angela Soler and Bradley Adams in the Forensic Anthropology Unit of the New York City Office of the Chief Medical Examiner. Although no new biogeochemical measurements were conducted in this study, NSF-CAREER (BCS-1455274) funding provided vital infrastructure and teaching opportunities that facilitated data integration and interpretation of existing records.

DATA AVAILABILITY STATEMENT

The data that support the findings of this study are available in the supplementary material of this article (see Data S1).

ORCID

Rhonda L. Quinn https://orcid.org/0000-0003-2580-864X

REFERENCES

- Alkass, K., Buchholz, B. A., Druid, H., & Spalding, K. L. (2011). Analysis of ¹⁴C and ¹³C in teeth provides precise birth dating and clues to geographical origin. Forensic Science International, 209(1–3), 34–41.
- Bartelink, E. J., & Chesson, L. A. (2019). Recent applications of isotope analysis to forensic anthropology. Forensic Sciences Research, 4, 29-44.
- Bergmann, O., Liebl, J., Bernard, S., Alkass, K., Yeung, M. S., Steier, P., Kutschera, W., Johnson, L., Landen, M., Druid, H., Spalding, K. L., & Frisen, J. (2012). The age of olfactory bulb neurons in humans. *Neuron*, 74, 634–639.
- Bernard, S., Frisen, J., & Spalding, K. L. (2010). A mathematical model for the interpretation of nuclear bomb test derived ¹⁴C incorporation in biological systems. Nuclear Instruments and Methods in Physics Research B, 268, 1295–1298.
- Broecker, S., Schulert, A., & Olson, E. (1959). Bomb carbon-14 in human beings. *Science*, 130, 331–332.
- Bronk, R. C. (2021). OxCal v4.4. https://c14.arch.ox.ac.uk
- Cerling, T. E., Barnette, J. E., Chesson, L. A., Douglas-Hamilton, I., Gobush, K. S., Uno, K. T., Wasser, S. K., & Xu, X. (2016). Radiocarbon dating of seized ivory confirms rapid decline in African elephant populations and provides insight into illegal trade. PNAS, 113, 13330– 12225.
- Cook, G. T., & MacKenzie, A. B. (2014). Radioactive isotope analyses of skeletal materials in forensic science: A review of uses and potential uses. *International Journal of Legal Medicine*, 128, 685–698.
- Cox, G., & Sealy, J. (1997). Investigating identity and life histories: Isotopic analysis and historical documentation of slave skeletons found on the Cape Town foreshore, South Africa. *International Journal of Historical Archaeology*, 1, 207–224.
- Fahy, G. E., Deter, C., Pitfield, R., Miszkiewicz, J. J., & Mahoney, P. (2017). Bone deep: Variation in stable isotope ratios and histomorphometric measurements of bone remodeling within adult humans. *Journal of Archaeological Science*, 87, 10–16.
- Fang, H., Deng, Z., Liu, J., Chen, S., Deng, Z., & Li, W. (2022). The mechanism of bone remodeling after bone aging. *Clinical Interventions in Aging*, 17, 405–415.
- Georgiadou, E., & Stenström, K. (2010). Bomb-pulse dating of human material: Modeling the influence of diet. *Radiocarbon*, *52*, 800–807.
- Geyh, M. A. (2001). Bomb radiocarbon dating of animal tissues and hair. Radiocarbon, 43, 723–730.

- Gocha, T. P., & Agnew, A. M. (2016). Spatial variation in osteon population density at the human femoral midshaft: Histomorphometric adaptation to habitual load environment. *Journal of Anatomy*, 228, 733–745.
- Hedges, R. E. M., Clement, J. G., Thomas, C. D. L., & O'Connell, T. C. (2007). Collagen turnover in the adult femoral mid-shaft: Modeled from anthropogenic radiocarbon tracer measurements. *American Journal of Physical Anthropology*, 133, 808–816.
- Heinemeier, K. M., Schjerling, P., Heinemeier, J., Magnusson, S. P., & Kjaer, M. (2013). Lack of tissue renewal in human adult Achilles tendon is revealed by nuclear bomb ¹⁴C. *The FASEB Journal*, 27, 2074–2079.
- Hillson, S. (1996). Dental anthropology. Cambridge University Press.
- Hodgins, G. W. L. (2009). Measuring atomic bomb-derived 14C levels in human remains to determine year of birth and/or year of death. US Department of Justice, National Institute of Justice August Report No.: 227839.
- Hua, Q., & Barbetti, M. (2004). Review of tropospheric bomb ¹⁴C data for carbon cycle modeling and age calibration purposes. *Radiocarbon*, 46, 1273–1298.
- Hua, Q., Barbetti, M., & Rakowski, A. (2013). Atmospheric radiocarbon for the period 1950–2010. *Radiocarbon*, 55, 2059–2072.
- Hua, Q., Turnbull, J. C., Santos, G. M., Rakowski, A. Z., Ancapichún, S., De Pol-Holz, R., Hammer, A., Lehman, S. J., Levin, I., & Miller, J. B. (2021). Atmospheric radiocarbon for the period 1950–2019. *Radiocarbon*, 64, 723–745.
- Ingle, B. M., Hay, S. M., Bottjer, H. M., & Eastell, R. (1999). Changes in bone mass and bone turnover following distal forearm fracture. Osteoporosis International, 10, 399–407.
- Johnstone-Belford, E., Fallon, S. J., Dipnall, J. F., & Blau, S. (2022a). Examining the use of different sample types following decomposition to estimate year of death using bomb pulse dating. *Journal of Forensic and Legal Medicine*, 85, 102275.
- Johnstone-Belford, E., Fallon, S. J., Dipnall, J. F., & Blau, S. (2022b). The importance of bone sample selection when using radiocarbon analysis in cases of unidentified human remains. Forensic Science International, 341, 111480.
- Johnstone-Belford, E. C., & Blau, S. (2020). A review of bomb pulse dating and its use in the investigation of unidentified human remains. *Journal* of Forensic Sciences, 65, 676–685.
- Kerstetter, J. E., Mitnick, M. E., Gundberg, C. M., Caseria, D. M., Ellison, A. F., Carpenter TO, & Insogna, K. L. (1999). Changes in bone turnover in young women cosuming different levels of dietary protein. The Journal of Climate Endocrinology & Metabolism, 84, 1052–1055.
- Kondo-Nakamura, M., Fukui, K., Matsu'ura, S., Kondo, M., & Iwadate, K. (2011). Single tooth tells us the date of birth. *International Journal of Legal Medicine*, 125, 873–877.
- Koon, H., & Tuross, N. (2013). The Dutch whalers: A test of a human migration in the oxygen, carbon and nitrogen isotopes of cortical bone collagen. World Archaeology, 45, 360–372.
- Lamb, A. L., Evans, J. E., Buckley, R., & Appleby, J. (2014). Multi-isotope analysis demonstrates significant lifestyle changes in king Richard III. Journal of Archaeological Science, 50, 559–565.
- Lehn, C., Rossmann, A., & Graw, M. (2015). Provenancing of unidentified corpses by stable isotope techniques—Presentation of case studies. Science and Justice, 55, 72–88.
- Libby, W. F., Berger, R., Mead, J. F., Alexander, G. V., & Ross, J. F. (1964). Replacement rates for human tissue from atmospheric radiocarbon. Science, 146, 1170–1172.
- Lynnerup, N., Kjeldsen, H., Heegaard, S., Jacobsen, C., & Heinemeier, J. (2008). Radiocarbon dating of the human eye lens crystallines reveal proteins without carbon turnover throughout life. PLoS One, 3, e1529.
- Martin, R. B. (2000). Toward a unifying theory of bone remodeling. *Bone*, 26, 1–6.
- Matsubayashi, J., & Tayasu, I. (2019). Collagen turnover and isotopic records in cortical bone. *Journal of Archaeological Science*, 106, 37–44.

- Meier-Augenstein, W., & Fraser, I. (2008). Forensic isotope analysis leads to identification of a mutilated murder victim. *Science & Justice*, 48, 153–159
- Naylor, K. E., Iqbal, P., Fledelius, C., Fraser, R. B., & Eastell, R. (2000). The effect of pregnancy on bone density and bone turnover. *Journal of Bone and Mineral Research*, 15, 129–137.
- Nydal, R. (1963). Increase in radiocarbon from the most recent series of thermonuclear tests. *Nature*, 200, 212–214.
- Nydal, R., & Lövseth, K. (1970). Prospective decrease in atmospheric radiocarbon. *Journal of Geophysical Research*, 75, 2271–2278.
- Parfitt, A. M. (2002). Misconceptions (2): Turnover is always higher in cancellous than in cortical bone. *Bone*, 30, 807–809.
- Parfitt, A. M. (2004). What is the normal rate of bone remodeling? *Bone*, 35, 1–3.
- Quinn, R. L., Alesbury, H., Ceja, L., Soler, A., & Godfrey, L. (2021). Food has no borders: Insights from the forensic isotopic profile of a New York City immigrant. Forensic Anthropology, 4, 14–25.
- Reimer, P., Austin, W., Bard, E., Bayliss, A., Blackwell, P., Bronk Ramsey, C., et al. (2020). The IntCal20 northern hemisphere radiocarbon age calibration curve (0–55 cal kBP). *Radiocarbon*, 62, 725–757.
- Reitsema, L. J., & Vercellotti, G. (2012). Stable isotope evidence for sexand status- based variations in diet and life history at medieval Trino Vercellese, Italy. American Journal of Physical Anthropology, 148, 589-600.
- Robling, A. G., Castillo, A. B., & Turner, C. H. (2006). Biomechanical and molecular regulation of bone remodeling. *Annual Review of Biomedical Engineering*, 8, 455–498.
- Scharlotta, I., Goriunova, O. I., & Weber, A. (2013). Micro-sampling of human bones for mobility studies: Diagenetic impacts and potentials for elemental and isotopic research. *Journal of Archaeological Science*, 40, 4509–4527.
- Sealy, J., Armstrong, R., & Schrire, C. (1995). Beyond lifetime averages: Tracing life histories through isotopic analysis of different calcified tissues from archaeological human skeletons. Antiquity, 69, 290–300.
- Shin, J. Y., O'Connell, T., Black, S., & Hedges, R. (2004). Differentiating bone osteonal turnover rates by density fractionation; validation using the bomb ¹⁴C atmospheric pulse. *Radiocarbon*, 46, 853–861.
- Spalding, K. L., Buchholz, B. A., Bergman, L.-E., Druid, H., & Fris en, J. (2005). Forensics: Age written in teeth by nuclear tests. *Nature*, 437, 333–334.
- Stenhouse, M. J., & Baxter, M. S. (1979). The uptake of bomb ¹⁴C in humans. In R. Berger & H. E. Suess (Eds.), *Radiocarbon dating* (pp. 324–341). University of California Press.
- Stenström, K. E., Skog, G., Georgiadou, E., Genberg, J., & Johansson, A. (2011). A guide to radiocarbon units and calculations (pp. 1–17). Lund University, Department of Physics internal report.
- Stout, S. D., & Lueck, R. (1995). Bone remodeling rates and skeletal maturation in three archaeological skeletal populations. *American Journal of Physical Anthropology*, 98, 161–171.
- Szpak, P., Metcalfe, J. Z., & Macdonald, R. A. (2017). Best practices for calibrating and reporting stable isotope measurements in archaeology. Journal of Archaeological Science: Reports, 13, 609-616.
- Taylor, R. E. (2000). Fifty years of radiocarbon dating. *American Scientist*, 88, 60–67.
- Ubelaker, D. H. (2014). Radiocarbon analysis of human remains: A review of forensic applications. *Journal of Forensic Sciences*, *59*, 1466–1472.
- Ubelaker, D. H., & Buchholz, B. A. (2005). Complexities in the use of bomb-curve radiocarbon to determine time since death of human skeletal remains. Forensic Science Communications, 8, 1–8.
- Ubelaker, D. H., Buchholz, B. A., & Stewart, J. E. B. (2006). Analysis of artificial radiocarbon in different skeletal and dental tissue types to evaluate date of death. *Journal of Forensic Sciences*, 51, 484–488.
- Ubelaker, D. H., & Parra, R. C. (2011). Radiocarbon analysis of dental enamel and bone to evaluate date of birth and death: Perspective from

- the southern hemisphere. Forensic Science International, 208, 103–107.
- Ubelaker, D. H., Plens, C. R., Pessoa Soriano, E., Vitor Diniz, M., de Almeida, J. E., Daruge Junior, E., Francesquini Junior, L., & Palhares Machado, C. E. (2022). Lag time of modern bomb-pulse radiocarbon in human tissues: New data from Brazil. Forensic Science International, 331, 111143.
- Ubelaker, D. H., Thomas, C., & Olson, J. E. (2015). The impact of age at death on the lag time of radiocarbon values in human bone. *Forensic Science International*, 251, 56–60.
- Uno, K. T., Quade, J., Fisher, D. C., Wittemyer, G., Douglas-Hamilton, I., Andanje, S., Omondi, P., Litoroh, M., & Cerling, T. (2013). Bomb-curve radiocarbon measurement of recent biologic tissues and applications to wildlife forensics and stable isotope (paleo)ecology. PNAS, 110, 11736-11741.
- Wild, E. M., Arlamovsky, K. A., Golser, R., Kutschera, W., Priller, A., Puchegger, S., Rom, W., Steier, P., & Vycudilik, W. (2000). 14C dating

with the bomb peak: An application to forensic medicine. *Nuclear Instruments and Methods in Physics Research*, 172, 944–950.

SUPPORTING INFORMATION

Additional supporting information can be found online in the Supporting Information section at the end of this article.

How to cite this article: Quinn, R. L. (2024). Bomb pulse ¹⁴C evidence for consistent remodeling rates of cortical femur collagen in middle-late adulthood. *American Journal of Biological Anthropology*, 1–18. https://doi.org/10.1002/ajpa.24887